

A H₂ PEM Fuel Cell and High Energy Dense Battery Hybrid Energy Source for an Urban Electric Vehicle

N. Schofield^{1#}, H. T. Yap¹ and C. M. Bingham²

^{1#}School of Electrical and Electronic Engineering, University of Manchester, M60 1QD, UK.

²Department of Electronic and Electrical Engineering, University of Sheffield, S1 3JD, UK

Corresponding Author

Abstract - Electric vehicles are set to play a prominent role in addressing the energy and environmental impact of an increasing road transport population by offering a more energy efficient and less polluting drive-train alternative to conventional internal combustion engine (ICE) vehicles. Given the energy (and hence range) and performance limitations of electro-chemical battery storage systems, hybrid systems combining energy and power dense storage technologies have been proposed for vehicle applications. The paper will discuss the application of a hydrogen fuel cell as a range extender for an urban electric vehicle for which the primary energy source is provided by a high energy dense battery. A review of fuel cell systems and automotive drive-train application issues are discussed, together with an overview of the battery technology. The prototype fuel cell and battery component simulation models are presented and their performance as a combined energy/power source assessed for typical urban and sub-urban driving scenarios.

I. INTRODUCTION

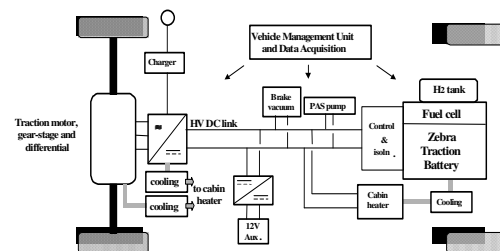
The impetus for more environmentally friendly road vehicles and alternative road vehicle energy conversion has fostered research and development in electrically powered vehicles for road transport applications since the late 1980's. This is particularly the case for medium to heavy-duty vehicles where some additional propulsion system mass is not as critical as for smaller passenger vehicles. Further, in recent years, fuel cell systems have also been proposed as a potential energy carrier, and the most suitable alternative likely to displace petroleum based fuels during the first half of this century [1,2]. Whilst there are many technical and resource management issues associated with the displacement of petroleum fuels for transportation, and the commensurate supply infrastructure requirements, this paper will discuss some of the application issues associated with the implementation of hybrid energy sources for electric and fuel cell vehicles. Specifically, the paper will report on initial drive-train design results from a research programme investigating the utility of an electric Taxi supplied via a high energy dense electro-chemical battery and hydrogen fuel cell range extender for inner city operation.

The aims of the research programme are to investigate and address the principal technical difficulties associated with the future commercial application of fuel cell technologies in electric vehicle traction drive-trains. As

such, a zero emission London taxi powered via two high peak power (32kW), high temperature, ZEBRA batteries and a 6kW, hydrogen, Proton Exchange Membrane fuel cell (PEMFC) system, is being developed for vehicle power-train test evaluation, as illustrated in Fig. 1 showing the vehicle and drive-train layout schematic. The prime mover for the taxi is a brushless permanent magnet (pm) machine and integrated gear reduction and differential drive to the vehicle back-axle. The pm machine is controlled via a three phase voltage source converter, the dc supply to which is provided by the traction battery and fuel cell via a dc:dc converter. The vehicle on-board hybrid energy source will allow the PEMFC to operate predominantly at a steady power, and at power levels associated with optimal fuel energy conversion efficiency, with the battery acting to buffer peak loads, recover vehicle braking energy and provide the bulk energy demand. Hence, the fuel cell operates primarily in a range extension function.



(a) London Taxi



(b) Drive-train schematic

Fig.1. Hydrogen fuel cell-high energy dense battery electric London Taxi and drive-train layout schematic.

The paper will review fuel cell systems and discuss automotive drive-train application issues, together with an overview of the battery technology. The regulation of the traction battery and fuel cell when subject to the dynamic power loading illustrated in Fig. 2(b),

necessitates detailed modelling to assess the functionality of the individual components once interconnected within the drive-train. Hence, the prototype fuel cell and battery component simulation models are presented and their performance as a combined hybrid energy source assessed for typical dynamic urban and sub-urban driving duty cycle scenarios. It is shown that the fuel cell and battery combination are complementary for such duty loading, extending the vehicle range whilst minimising the installed fuel cell power.

II. VEHICLE ENERGY AND POWER REQUIREMENTS

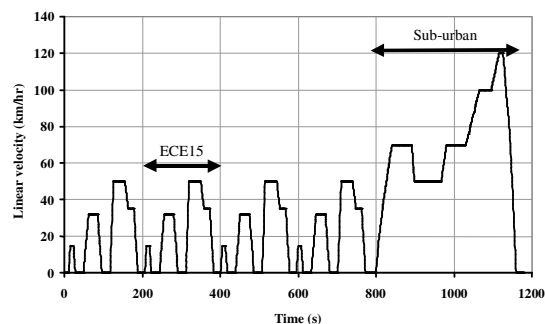
For road vehicle applications, the on-board energy and power sources must satisfy the load demand of the vehicle traction drive-train. The decision as to whether the energy storage medium supplies all of the vehicle load or simply the average power requirements can significantly influence the sizing of the vehicle energy/power systems and hence system cost. The difficulty in making this assessment is in choosing the most appropriate duty rating specification for the vehicle. For example, Fig. 1 illustrates a typical 2.5 tonne urban electric vehicle, a London Taxi, which is the reference vehicle for the study. The power required to propel the vehicle over the NEDC driving cycle, Fig. 2(a), that comprises of 4x enhanced European Commission R15.04 (ECE15) urban cycles and 1x EC sub-urban cycle [1,2], is detailed in Table I, showing a wide disparity in peak-to-average power requirements, i.e. 17:1 and 4:1 for the urban and sub-urban profiles respectively.

Table I. Vehicle power requirement.

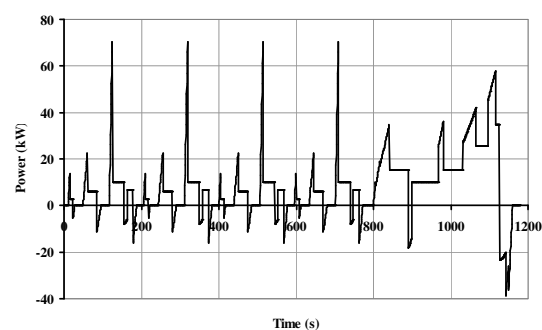
Driving cycle	Power condition	Cycle time (s)	Range (km)	Power (kW)
ECE15	Max. motoring	195	1.13	70.35
	Max. regenerating			-16.16
	Average			4.21
Sub-urban	Max. motoring	400	6.96	57.84
	Max. regenerating			-38.83
	Average			14.57
NEDC	Average	1180	11.47	7.72

The data in Table I is calculated via solution of the vehicle kinematics [3] with the NEDC linear velocity driving cycle of Fig. 2(a). The vehicle parameter data for the Taxi is given in Appendix I. The vehicle dynamic power profile calculated over the NEDC driving cycle is illustrated in Fig. 2(b), and used for subsequent vehicle performance assessment. There is also a similar disparity in the vehicle peak-average power for other driving (or duty) cycles, i.e. the Highway fuel economy test schedule (HWFET), US 1975 schedule (FTP75) and Japanese 11-mode test schedule, hence the potential to over-size the vehicle energy source for single source systems, as discussed in [4]. Note, that whilst all sources are a source of energy,

reference is made here to energy and power to emphasise the functionality of the vehicle on-board sources with respect to the vehicle energy management philosophy.



(a) NEDC (4x ECE15 + sub-urban) driving cycle



(b) Vehicle power vs. time

Fig.2. Vehicle linear velocity and associated dynamic power requirements for the London Taxi.

III. FUEL CELLS FOR TRANSPORTATION

A. Background

A major advantage of fuel cell powered vehicles is the development of cleaner, more energy efficient cars, trucks, and buses that can initially operate on conventional fuels via local reformation, i.e. gasoline and diesel, whilst enabling the technology platform for a future move to renewable and alternative fuels, i.e. methanol, ethanol, natural gas, and other hydro-carbons, and ultimately hydrogen, a particularly significant issue when considering the infrastructure and support requirements of a modern transportation network.

With on-board fuels other than pure hydrogen, for example, natural gas, methanol and gasoline, the fuel cell systems could use an appropriate fuel processor to convert the fuel to hydrogen. Since the fuel cell relies on chemistry and not combustion, local emissions from this type of a system should, potentially, be much smaller than emissions from the cleanest fuel combustion process emissions, whilst offering the advantages of an electric transmission. However, in traction systems, fuel cells have major operational disadvantages in terms of their voltage regulation and inability to accept vehicle kinetic energy during braking

[5,6], hence the consideration of a hybrid energy/power source.

For the taxi vehicle test platform, 2x 3kW PEM fuel cells have been chosen to provide a background energy input, essentially acting as a vehicle range extender. The fuel cells are prototype systems developed by MES-DEA, Switzerland [5], and are designed to realise a very compact, lightweight and simple fuel stack. The stack has separate forced air flow systems for cooling and reaction air supply, operate close to ambient pressure on the cathode for seal integrity, have a modular layout, but most significantly, has no auxiliary humidification components. A microprocessor manages the associated cooling and air flow fans, steering electronics for membrane hydration, main and purge valves. Fig. 3 illustrates the 3kW prototype fuel cell system and control electronics, the main specification details of which are given in Appendix I [5].

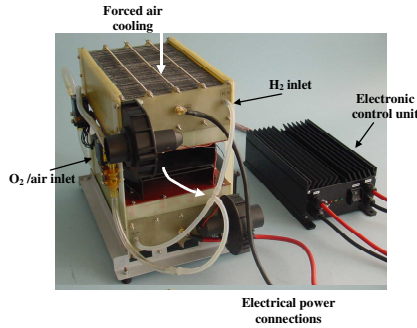


Fig.3. Prototype fuel cell system and control electronics [5].

B. Fuel Cell Modelling

As with electro-chemical batteries, fuel cells exhibit non linear performance characteristics that can significantly influence vehicle drive system operation and component optimisation if not considered at the system design stage. The three main fuel cell loss mechanisms, can be summarised as:

- irreversible/activation polarisation loss,
- concentration polarisation loss , and
- ohmic or resistance polarisation.

The influence of these loss mechanisms on fuel cell performance is illustrated in Fig. 4, showing measured fuel cell voltage and power output as a function of cell current density (or load current). The fuel cell can be modelled by a semi-empirical equation as discussed in [7] for which parameters are calculated through an identification process with experimental data, viz.:

$$V_{cell} = E_o - b \ln(J) - (R_{int} J) - k_1 e^{(k_2 J)} \quad (1)$$

The equation terms are derived from the associated Nernst, Tafel and Ohm's laws, where V_{cell} is the fuel cell terminal voltage E_o is the steady open-circuit voltage, b is the Tafel's parameter for oxygen reduction, J the current density, R_{int} the cell ohmic resistance and k_1 and k_2 diffusion parameters. Whilst the model is not universal with regard to the fuel cell fundamental

chemistry, it is much simpler in form and represents the main voltage loss components. Each term in (1) is dominant in each region of the V - J characteristic. In region A, the cell voltage decreases drastically due to the oxygen electrochemical activation reactions, where the logarithm term has the main influence. In region B, the curve is roughly linear, i.e. essentially ohmic resistive losses, and Region C corresponds to diffusion losses, i.e. exponential term. The five parameters in (1) depend on cell temperature and gas pressures. However, for the fuel cell stack considered, the stack temperature is tightly regulated via forced ventilation and the stack pressure is fixed to 1.4bar. Fig. 4 shows measured voltage regulation and power capacity with load current for a 3kW MES-DEA fuel cell.

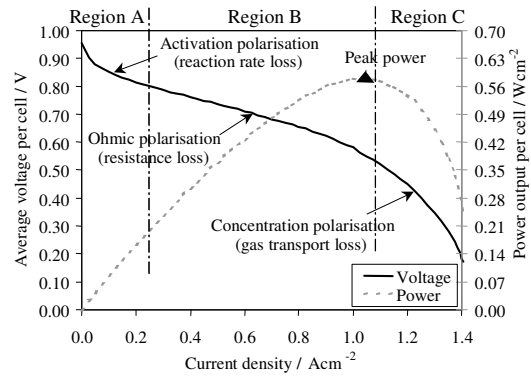


Fig.4. Measured voltage and power data for MES-DEA H₂ PEM fuel cell [2].

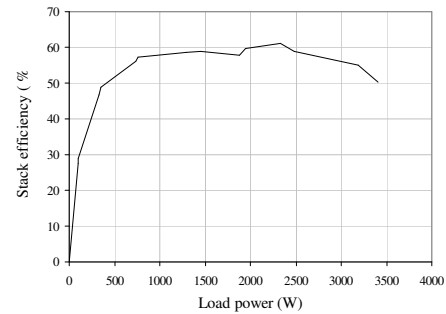


Fig.5. Measured fuel cell stack hydrogen-to-electrical energy efficiency with output load.

For modelling purposes, implementation of (1) can be problematic at zero current; hence a simpler quadratic fit to the measured data of Fig. 3 is used:

$$V_{cell} = k_a + k_b J + k_c J^2 + k_d J^3 + k_e J^4 + k_f J^5 + k_g J^6 + k_h J^7 + k_i J^8 + k_j J^9 + k_k J^{10} \quad (2)$$

where V_{cell} is the fuel cell terminal voltage per cell, and J the cell current density. The fuel cell terminal voltage is used in conjunction with the measured stack fuel-to-electrical conversion efficiency, as illustrated in Fig. 5, to simulate operation and predict performance. Again, a

curve fit to the measured data of Fig. 5 is used in the fuel cell model:

$$\eta = a_a + a_b P_{\%}^{0.5} + a_c P_{\%} + a_d P_{\%}^{1.5} + a_e P_{\%}^2 + a_f P_{\%}^{2.5} \quad (3)$$

where η is the fuel efficiency and $P_{\%}$ the fuel cell per unit load power, and the parameter values for (2) and (3) are as given in Appendix I.

C. Fuel Cell Operation

For road vehicle applications, the fuel cell (FC) system must satisfy or contribute to the load demand of the vehicle traction drive-train. The decision as to whether the FC system supplies all of the vehicle load or simply the average energy requirements can significantly influence the sizing of the FC system and hence the FC system cost. A vehicle supplied solely via fuel cells would necessitate operation at low current densities (and hence over-sizing of the FC) to minimise the voltage swing on the dc supply to the vehicle traction system. Hence, the taxi vehicle considered were the variation in peak-average power demand is 17:1 and 4:1 respectively for urban and sub-urban driving, the fuel cell system would have to be rated much higher than the peak power specified. Additionally, since fuel cells cannot accept vehicle kinetic energy during braking, some form of transient power buffer can significantly reduce the installed fuel cell power capacity [4]. Note, the time-transient response of the FC fuelling also fosters FC operation in a hybrid-energy source configuration.

There are, therefore, clear benefits in terms of FC size and the recovery of vehicle regenerative braking energy for operation of FC systems in hybrid energy source configurations, where the FC supplies the vehicle average energy, or provides a range extension/battery support function, in combination with a peak power buffer, such as supercapacitor or, as for the taxi, a higher power dense battery.

IV. VEHICLE TRACTION BATTERY

A. Background

The ZEBRA technology is a serious candidate to power future electric vehicles since it not only has an energy density $\sim 2.5x$ that of lead acid batteries (50% more than NiMH) but also has a relatively flat Peukert characteristic from 0 to 80% depth-of-discharge (DOD), has good power density for acceleration and acceptance of regenerative energy, no maintenance, essentially intolerant to external temperature ambient, safety and fault tolerance, and, perhaps of greatest significance for the automotive sector, the potential for low cost in volume manufacture. Originally developed by Beta R&D in the UK, the ZEBRA battery technology is now owned and manufactured by MES-DEA, Switzerland. Commercialisation of the battery has made considerable progress in recent years, particularly in the automation of assembly and component optimisation. Production is

2000 batteries per year with planned staged increases in capacity to 33,000 batteries, and with space available on site for a further expansion to a maximum of 100,000 batteries [8]. The ZEBRA battery system has been used in many applications, including electric vehicles. So far, the batteries had been installed in cars, buses and vans from Mercedes, BMW, Opel, VW, Renault, Fiat, MAN, Evobus, IVECO, Larag and Autodromo [9].

For the taxi traction system, a nominal dc link of 550V was chosen to minimise the electrical power distribution mass and fully utilise the traction inverter silicon volt-ampere rating. The dc link voltage is realised via 2x Z5C traction batteries, Fig. 6, electrically connected in series, details of which are given in Appendix I [10].



Fig.6. ZEBRA Z5C Traction battery.

B. Zebra Battery Simulation Model

Electric vehicle traction duties are typified by high power discharge/charge rates for vehicle acceleration and braking demands respectively [3,4], as illustrated by Fig. 2(b). Since the traction battery supplies the vehicle traction drive-system, the battery voltage regulation with load current is an important aspect of vehicle operation and system performance modelling. Simulation of the ZEBRA battery is facilitated via a detailed analytic model employing non-linear open-circuit terminal voltage and resistance characteristics derived from cell experimental test data provided by Beta R&D. Since the battery dynamic current loadings are of a relatively low frequency ($<100\text{Hz}$ for the NEDC cycle), the battery equivalent circuit model can be simplified to that illustrated in Fig. 7(a). The open-circuit terminal voltage of the battery depends on battery state-of-charge (SoC), or discharged ampere-hour, and is found to be independent of load current, Fig. 7(b). The specified maximum discharge ampere-hour (Ah) capacity is taken from the manufacturer's nameplate capacity and collaborated via a series of Peukert tests. The battery internal resistance is similarly determined from test and is a function of discharged Ah and charging/discharging current rate, Fig. 7(c).

As with the fuel cell model, functions for the ZEBRA battery open-circuit voltage and internal resistance are derived from curve-fits to measured battery test data. These analytic expressions thus improve on simulation time when solving multiple component drive-train models. The curve fit equations and battery model parameters are given in Appendix II.

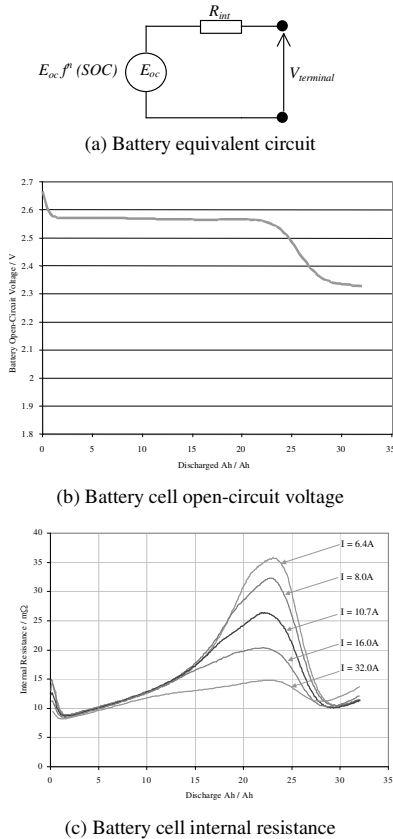


Fig. 7. ZEBRA Z5C battery cell equivalent circuit model and model parameter characteristics.

C. Lead-acid Battery Simulation Model

As a comparison of two vehicle battery technologies at the initial vehicle component assessment and specification stage, a similar model is implemented for a sealed lead-acid battery, as discussed in [4]. The lead-acid battery details are provided in Appendix I.

V. VEHICLE PERFORMANCE EVALUATION

As previously discussed, the two major operational problems with fuel cell systems in electric vehicle drive-trains is their poor regulation with load, Fig. 4, and inability to accept regenerative currents which, if allowed, would result in excessive chemical fatigue of the stack membranes and hence reduced life-time [5]. Consequently, if the fuel cell system mass and volume is to be kept within limits commensurate with their utility in the drive-train, some form of peak power buffering is necessary and hence a hybrid energy source for the vehicle.

The energy management strategy considered for the taxi vehicle is one where the fuel cell provides a range extension function supplementing the battery energy, whilst allowing all dynamic power demands to be taken by the battery. As an assessment of the on-board energy

sources the taxi performance was evaluated via two duty loading regimes, viz.:

- repetitive ECE15 cycles, i.e. inner city driving, and the more energy demanding,
- repetitive NEDC cycles.

The battery management strategy chosen ensures operation within nameplate voltage and current limits, the minimum voltage limit dictating actual energy utilisation, and hence operating time and range. The fuel cell utilisation was constrained by the quoted on-board hydrogen storage. However, the fuel cell stack was considered as providing a light mean supply of 2kW and a mean supply of 4kW, hence, operating over the most energy conversion efficient region of the stack, Fig. 5. A number of case studies were considered; Cases 1-4 being for pure battery mode and comparing the ZEBRA and more common sealed lead-acid technologies; Cases 5 and 6 assess the performance of the combined ZEBRA battery and fuel cell source. Part (i) of Table II provides the test conditions and battery details for each case, whilst parts (ii) and (iii) give the simulated data for the two duty cycle regimes.

A. Pure battery electric mode

For both duty regimes, Case 1 gives results for the ZEBRA battery, whilst Case 2 compares the lead-acid performance for the same battery mass as that of the ZEBRA, Case 3 for the same battery volume and Case 4 for the same nameplate energy. These results clearly highlight the benefits of the ZEBRA battery in terms of mass and volume, showing an increased range of 2.4x based on mass and 1.4x based on volume. From a vehicle system point of view, minimisation of vehicle on-board mass is the primary goal since this equates to drive-train peak power rating. Whilst component volume is important, it is not as critical for the taxi example given the available vehicle space envelope. The result of Case 4 has been included for interest, but such a mass impact would compromise the vehicle functionality by significantly limiting passenger payload. It is worth noting that the lead-acid simulation assumed a constant battery coolant ambient of 20°C which would, in practice, necessitate a thermal management system, figures for which are not included in the mass and volume audits. Fig. 8 illustrates simulated battery terminal voltage variation for the repetitive NEDC duty loading, for the Zebra battery (a), and the lead-acid battery (b), corresponding to Cases 1 and 2 respectively.

B. Fuel cell and battery hybrid source

Cases 5 and 6 compare vehicle performance with a mean fuel cell input of 2 and 4kW respectively. The results of Table II demonstrate the benefit of the additional energy source in extending the vehicle range, in both cases by a factor of 2, making the vehicle operating times and range attractive for fleet taxi schemes.

Table II. Vehicle performance evaluation

Case	Battery	Battery rated capacity (Ah)	Total battery No	Total battery	
				Volume (l)	Mass (kg)
1	Z5C	66.0	2	266.4	390.0
2	Pb-acid	31.3	36	157.6	390.0
3	Pb-acid	52.9	36	266.4	658.4
4	Pb-acid	73.5	36	365.0	914.8
5	Z5C+FC	66.0	2	266.4	390.0
6	Z5C+FC	66.0	2	266.4	390.0

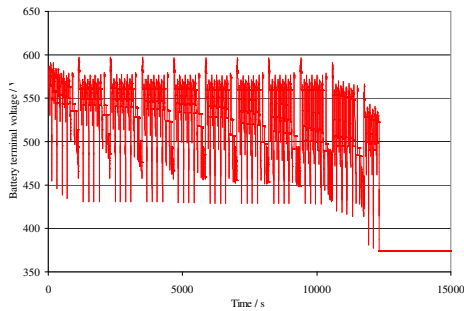
(ii) Repetitive ECE15 cycles

	Battery	Ave. FC power (kW)	Time duration (hrs)	Range (km)
1	Z5C	0	5.79	126.7
2	Pb-acid	0	2.48	51.7
3	Pb-acid	0	4.22	87.9
4	Pb-acid	0	5.75	119.9
5	Z5C+FC	2	10.46	218.0
6	Z5C+FC	4	11.95	249.0

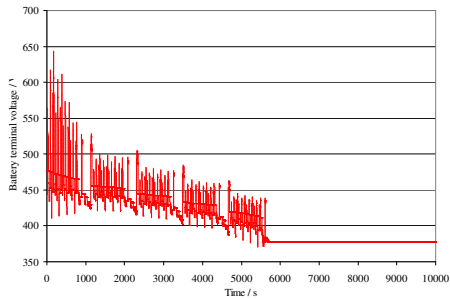
(iii) Repetitive NEDC cycles

	Battery	Ave. FC power (kW)	Time duration (hrs)	Distance (km)
1	Z5C	0	3.42	119.8
2	Pb-acid	0	1.58	32.9
3	Pb-acid	0	2.56	89.8
4	Pb-acid	0	3.42	119.8
5	Z5C+FC	2	4.63	161.9
6	Z5C+FC	4	6.92	242.2

Per cycle values	Duration (s)	Distance (km)
ECE15	195	1.129
NEDC	1180	11.471



(a) ZEBRA battery



(b) Lead-acid battery

Fig.8. Simulated battery terminal voltage vs. time for repetitive NEDC duty cycles.

VI. CONCLUSIONS

The paper has reviewed fuel cell systems for transportation and discussed the main application issues in automotive drive-trains, specifically their poor voltage regulation with load and inability to accept regenerative braking energy. A detailed model of a prototype fuel cell and ZEBRA traction battery suitable for vehicle performance simulation has been presented and vehicle performance assessed for various battery and fuel cell combinations, and for typical dynamic urban and sub-urban driving duty cycle regimes. It has been shown that the fuel cell and battery combination are complementary for such duty loading, extending the vehicle range whilst minimising the installed fuel cell capacity. The results demonstrate the utility of combining energy and power sources for electric vehicle propulsion.

ACKNOWLEDGMENTS

The authors acknowledge the support of the UK Engineering and Physical Science Research Council (EPSRC), via Grant No. GR/S81971/01; SEMELAB PLC, UK, for provision of a research studentship and Beta R&D, Derby, UK, for provision of test data and technical information.

REFERENCES

- [1] N. Schofield, H.T. Yap, G. Maggeto, P. Van den Bossche, and J. Van Mierlo, "A state-of-the-art review and database of fuel cells and their application in electric vehicles useful for education needs", Proc. 10th European Conf. on Power Electronics and Applications (EPE2003), CD ROM, Paper 906, pp. 1-10, Sept. 2003.
- [2] Thematic Network on 'Fuel Cells, Electric and Hybrid Vehicles (ELEDRIE)', a Network funded under Framework V, Contract No. ENK6-CT-2000-20057, Project No. NNE5-1999-20036.
- [3] N. Schofield, C.M. Bingham, and D. Howe, "Regenerative braking for all-electric and hybrid electric vehicles", IMechE Conf. Braking 2002, Leeds, UK, pp. 175-183, July 2002.
- [4] H.T. Yap, N. Schofield, and C.M. Bingham, "Hybrid energy/power sources for electric vehicle traction systems", IEE PEMD Conference, pp. 1-6, May 2004.
- [5] MES-DEA, Fuel Cell Systems, Technical Information, Switzerland, 2003.
- [6] A.J. Appleby, and F.R. Foulkes, "Fuel Cell Handbook", Book, Van Nostrand Reinhold, 1989.
- [7] S. Busquet, C.E. Hubert, J. Labbe, D. Mayer, and R. Metkemeijer, "A new approach to empirical electrical modelling of a fuel cell, an electrolyser or a regenerative fuel cell", Journal of Power Sources, vol. 134, pp. 41-48, 2004.
- [8] Cord-H. Dustmann, "Zebra battery meets USABC goals", Journal of Power Sources, vol. 72, pp.27-31, 1998.
- [9] J. Sudworth, "The sodium/nickel chloride (ZEBRA) battery", Journal of Power Sources, vol. 100, pp. 149-163, 2001.
- [10] Zeb5 component data, Beta R&D, Derby, UK, 2003.

APPENDIX I: MODEL DATA AND
COMPONENT SPECIFICATIONS

London Taxi Vehicle Data

Gross vehicle weight	2500 kg
Drag force coefficient	0.31
Equivalent frontal area	1.75m ²
Coefficient of rolling resistance	0.03
Road wheel radius	0.274 m
Wheel inertia	0.164 kgm ²
Traction machine inertia	0.57x10 ⁻³ kgm ²

MES-DEA 3.0kW prototype fuel cell system [5]

Performance data	
Unreg. dc output voltage range	72 - 114V
H ₂ consumption at full-load	39ln/min. (0.2kg/h)
Max. power output	3kW
Open circuit voltage per cell	0.95V
Number of cells per stack	120
Active cell area	61cm ²
Operating conditions	
Stack temperature	Max. 63°C
Hydrogen pressure	0.4-0.7 bar
Air pressure	Ambient
Fuel supply	Pure hydrogen, dead-end mode
Ambient temperature	0 to +35°C
Gas humidification	none
Working cycle	continuous
Cooling	Force air cooled
Stack volume	410 x 305 x 235 mm
Control unit volume	295 x 155 x 95 mm
Stack weight	9kg
System weight	11kg
Vehicle on-board Hydrogen storage	
Gas storage	Compressed H ₂ at 230bar
Storage medium	3x carbon composite cylinders
Total storage capability	90litres

ZEBRA Z5C battery data [9]

Type	Zebra Z5C
Capacity	66Ah
Rated energy	17.8kWh
Open circuit voltage	278.6V
Max. regen voltage	335V
Max. charging voltage	308V
Min. voltage	186V
Max. discharge current	224A
Weight	195kg
Specific energy	91.2Wh/kg
Specific power	164W/kg
Peak power	32kW
Thermal Loss	<120W
Cooling	Air
Battery internal temperature	270 to 350°C
Ambient temperature	-40 to +70°C
Dimensions (WxLxH)	533 x 833 x 300 mm
Number of cells per battery	216
Cell configuration	2 parallel strings of 108 series cells

Fuel Cell Model Parameters:

Parameters for equation (2):		Parameters for equation (3):	
k_a	0.950602847	a_a	-0.000558716
k_b	-2.111185823	a_b	1.196398539
k_c	18.4080918	a_c	4.580251356
k_d	-101.455289	a_d	-17.6473079
k_e	333.775762	a_e	20.45606645
k_f	-684.4227687	a_f	-8.028431982
k_g	892.8408354		
k_h	-737.7160864		
k_i	371.7575573		
k_j	-103.5699007		
k_k	12.12124403		

Sealed lead-acid battery data

Model	HAWKER Genesis EP Series
Cell number	6 cells per module
Nominal voltage	12V (2V per cell)
Max. voltage	13.5V open circuit (2.25V per cell)
Max. charging voltage	16V (2.67V per cell)
Min. voltage	10.2V (recommended, 1.7V per cell)
Max. current	450A
Rated energy	0.1318 to 0.846kWh
Rated capacity	70Ah
Rated temperature	20°C
Mass	24.2kg
Volume	9.79l
Dimension	331mm x 168mm x 176mm

APPENDIX II: ZEBRA EQUIVALENT CIRCUIT MODEL

The following equations model the ZEBRA battery as a function of discharge Ampere-hour (q) and battery terminal supply current (i). The equation for cell open-circuit voltage is given by:

$$E_{oc} = \frac{v_a + v_c q^{0.5} + v_e q^1 + v_g q^{1.5} + v_i q^2 + v_k q^{2.5}}{1 + v_b q^{0.5} + v_d q^1 + v_f q^{1.5} + v_h q^2 + v_j q^{2.5}} \quad (A1)$$

From experimental test data, the battery internal resistance is found to be a complex function of discharge ampere-hour (or SoC) and current charge/discharge rate. Curve fit functions are used to analytically model the internal resistance. However, due to highly non-linear relationship, it is not possible to fit one 3-dimension equation to the full data set without the model losing accuracy. To overcome this problem, the model uses a set of eleven equations determined by the current rate and discharge ampere-hour. For example, for discharge currents higher than 40A, a constant resistance of R_{max-2} is used. For all other regions, i.e. when discharge current is between 0A to 40A, the appropriate resistance equation is chosen according to the defined conditions.

The choice of battery cell internal resistance is dictated by the following algorithm:

Loop start

if ' $q > ah_{ref}$ ' then 'simulation stop' else

if ' $i \leq 0$ ' then ' $r_{int} = r_{chg}$ ' else

if ' $i > 40$ ' then ' $r_{int} = r_{max-2}$ ' else

if ' $i \leq 15$ and $q \leq 2$ ' then ' $r_{int} = r_{a0}$ ' else

if ' $i > 15$ and $q \leq 2$ ' then ' $r_{int} = r_{al}$ ' else

if ' $26 < q < 28$ ' then ' $r_{int} = r_{d0}$ ' else

if ' $q \leq 15$ and $2 < i \leq 28$ ' then ' $r_{int} = r_{b0}$ ' else

if ' $q > 15$ and $2 < i \leq 5$ ' then ' $r_{int} = r_{b1}$ ' else

if ' $q > 15$ and $5 < i \leq 22.5$ ' then ' $r_{int} = r_{b3}$ ' else

if ' $q > 15$ and $22.5 < i \leq 28$ ' then ' $r_{int} = r_{b2}$ ' else

if ' $q \leq 15$ and $i > 28$ ' then ' $r_{int} = r_{c0}$ ' else

if ' $q > 15$ and $i > 28$ ' then ' $r_{int} = r_{cl}$ '

if ' $r_{int} > r_{max}$ ' then ' $r_{int} = r_{max}$ '

Loop end

$$R_{A1} = \frac{a_{1a} + a_{1b}q + a_{1c}q^2 + a_{1d}i}{1 + a_{1e}q + a_{1f}q^2 + a_{1g}i} \quad (A2)$$

$$R_{B0} = \frac{b_{0a} + b_{0b}q + b_{0c}q^2 + b_{0d}i}{1 + b_{0e}q + b_{0f}q^2 + b_{0g}i} \quad (A3)$$

$$R_{B1} = \frac{b_{1a} + b_{1b}q + b_{1c}q^2 + b_{1d}i}{1 + b_{1e}q + b_{1f}q^2 + b_{1g}i} \quad (A4)$$

$$R_{B2} = \frac{b_{2a} + b_{2b}q + b_{2c}q^2 + b_{2d}q^3 + b_{2e} \ln i}{1 + b_{2f}q + b_{2g} \ln i} \quad (A5)$$

$$R_{B3} = \frac{b_{3a} + b_{3b}q + b_{3c}q^2 + b_{3d}q^3 + b_{3e}i}{1 + b_{3f}q + b_{3g}q^2 + b_{3h}i} \quad (A6)$$

Hence, the equations used to calculate the cell internal resistance, R_{int} , in m Ω are:

$$R_{C1} = \frac{c_{1a} + c_{1b}q + c_{1c}q^2 + c_{1d}q^3 + c_{1e} \ln i}{1 + c_{1f}q + c_{1g}q^2 + c_{1h}q^3 + c_{1i} \ln i} \quad (A7)$$

$$R_{A0} = a_{0a} + \frac{4a_{0b}e^{\left(\frac{q-a_{0c}}{a_{0d}}\right)}}{\left[1 + e^{\left(\frac{q-a_{0c}}{a_{0d}}\right)}\right]^2} + \frac{4a_{0e}e^{\left(\frac{i-a_{0f}}{a_{0g}}\right)}}{\left[1 + e^{\left(\frac{q-a_{0c}}{a_{0d}}\right)}\right]^2} + \frac{16a_{0h}e^{\left(\frac{(q-a_{0c})}{a_{0d}}\right)\left(\frac{i-a_{0f}}{a_{0g}}\right)}}{\left[1 + e^{\left(\frac{q-a_{0c}}{a_{0d}}\right)}\right]^2 \left[1 + e^{\left(\frac{q-a_{0f}}{a_{0g}}\right)}\right]^2} \quad (A8)$$

$$R_{C0} = c_{0a} + \frac{c_{0b}}{q} + \frac{c_{0c}}{i} + \frac{c_{0d}}{q^2} + \frac{c_{0e}}{i^2} + \frac{c_{0f}}{qi} + \frac{c_{0g}}{q^3} + \frac{c_{0h}}{i^3} + \frac{c_{0i}}{qi^2} + \frac{c_{0j}}{q^2i} \quad (A9)$$

$$R_{D0} = d_{0a} + d_{0b} \ln q + d_{0c} \ln i + d_{0d} [\ln q]^2 + d_{0e} [\ln i]^2 + d_{0f} [\ln q][\ln i] + d_{0g} [\ln q]^3 + d_{0h} [\ln i]^3 + d_{0i} [\ln q][\ln i]^2 + d_{0j} [\ln q]^2 [\ln i] \quad (A10)$$

Zebra battery model parameter values

v_a	2.668550131	d_{0h}	0.524300703	b_{0a}	8.538290542	b_{2e}	-5.216032308	c_{0h}	-3848.834185
v_b	-2.161541495	d_{0i}	-22.38078476	b_{0b}	-0.424796912	b_{2f}	0.002232179	c_{0i}	-11139.14849
v_c	-5.768152987	d_{0j}	-412.8784228	b_{0c}	0.00482931	b_{2g}	-0.452954018	c_{0j}	1204035.646
v_d	2.47814445	a_{0a}	8.29672091	b_{0d}	0.035452834	b_{3a}	7.344557606	c_{1a}	12.19982394
v_e	6.543581931	a_{0b}	2.654229606	b_{0e}	-0.08078068	b_{3b}	-0.226075522	c_{1b}	-1.200804369
v_f	-0.94931541	a_{0c}	0.177295354	b_{0f}	0.001643179	b_{3c}	-0.02883916	c_{1c}	0.03939517
v_g	-2.50604762	a_{0d}	0.241852423	b_{0g}	0.00500249	b_{3d}	0.001220193	c_{1d}	-0.000431123
v_h	0.14455723	a_{0e}	0.653017062	b_{1a}	8.224355635	b_{3e}	0.031523757	c_{1e}	0.005384114
v_i	0.383236649	a_{0f}	7.390945256	b_{1b}	-0.307842076	b_{3f}	-0.10240466	c_{1f}	-0.098137889
v_j	-0.007606508	a_{0g}	1.661911031	b_{1c}	0.001595691	b_{3g}	0.002643072	c_{1g}	0.003212432
v_k	-0.020331713	a_{0h}	2.974473025	b_{1d}	0.053949783	b_{3h}	0.004302133	c_{1h}	-3.50917E-05
d_{0a}	100888.7072	a_{1a}	12.8420689	b_{1e}	-0.077968772	c_{0a}	-1110.598606	c_{1i}	0.000354365
d_{0b}	-84923.67774	a_{1b}	-18.48590873	b_{1f}	0.001550886	c_{0b}	105087.9293	Ah_{ref}	0 to 34
d_{0c}	-5137.577354	a_{1c}	20.68546045	b_{1g}	0.007381905	c_{0c}	943.1554737	R_{max}	80.0
d_{0d}	23809.05796	a_{1d}	0.03576463	b_{2a}	481.9178496	c_{0d}	-3236953.626	R_{max-2}	7.5
d_{0e}	72.46775398	a_{1e}	-1.663449676	b_{2b}	-56.51569106	c_{0e}	1695.83145	R_{chg}	5.0
d_{0f}	2917.312426	a_{1f}	2.272354708	b_{2c}	2.238986889	c_{0f}	-72760.13798		
d_{0g}	-2223.104357	a_{1g}	0.011695949	b_{2d}	-0.029265742	c_{0g}	32930698.08		